Gramicidin-perforated Patch Recording Revealed the Oscillatory Nature of Secretory Cl^- Movements in Salivary Acinar Cells

Makoto Sugita, Chikara Hirono, and Yoshiki Shiba

Department of Oral Physiology, Graduate School of Biomedical Sciences, Hiroshima University, Hiroshima 734-8553, Japan

ABSTRACT Elevations of cytoplasmic free calcium concentrations ($[Ca^{2+}]_i$) evoked by cholinergic agonists stimulate isotonic fluid secretion in salivary acinar cells. This process is driven by the apical exit of Cl^- through Ca^{2+}-activated Cl^- channels, while Cl^- enters the cytoplasm against its electrochemical gradient via a loop diuretic-sensitive Na^+-K^+-$2Cl^-$ cotransporter (NKCC) and/or parallel operations of Cl^--HCO_3^- and Na^+-H^+ exchangers, located in the basolateral membrane. To characterize the contributions of those activities to net Cl^- secretion, we analyzed carbachol (CCh)-activated Cl^- currents in submandibular acinar cells using the "gramicidin-perforated patch recording configuration." Since the linear polypeptide antibiotic gramicidin creates monovalent cation-selective pores, CCh-activated Cl^- currents in the gramicidin-perforated patch recording were carried by Cl^- efflux via Cl^- channels, dependent upon Cl^- entry through Cl^- transporters expressed in the acinar cells. CCh-evoked oscillatory Cl^- currents were associated with oscillations of membrane potential. Bumetanide, a loop diuretic, decreased the CCh-activated Cl^- currents and hyperpolarized the membrane potential. In contrast, neither methazolamide, a carbonic anhydrase inhibitor, nor elimination of external HCO_3^- had significant effects, suggesting that the cotransporter rather than parallel operations of Cl^--HCO_3^- and Na^+-H^+ exchangers is the primary Cl^- uptake pathway. Pharmacological manipulation of the activities of the Ca^{2+}-activated Cl^- channel and the NKCC revealed that the NKCC plays a substantial role in determining the amplitude of oscillatory Cl^- currents, while adjusting to the rate imposed by the Ca^{2+}-activated Cl^- channel, in the gramicidin-perforated patch configuration. By concerting with and being controlled by the cation steps, the oscillatory form of secretory Cl^- movements may effectively provide a driving force for fluid secretion in intact acinar cells.

KEY WORDS: chloride secretion • exocrine glands • chloride channels • cation–chloride cotransporter • gramicidin

INTRODUCTION

Cholinergic agonists trigger several forms of $[Ca^{2+}]_i$ signals in exocrine acinar cells, which include $[Ca^{2+}]_i$ oscillations and Ca^{2+} waves, that are governed by the action of Ca^{2+} channels and Ca^{2+} pumps (Gray, 1988; Lee et al., 1997a,b). The elevation of $[Ca^{2+}]_i$ stimulates fluid secretion by activating ion permeabilities (Foskett and Melvin, 1989; Petersen, 1992; Turner, 1993). Importantly, fluid secretion requires the polarized distribution of ion channels and transporters (He et al., 1997). Ca^{2+}-activated Cl^- channels in the apical membrane as well as Ca^{2+}-activated K^+ channels in the basolateral membrane are believed to be essential for fluid secretion in the salivary glands (Petersen, 1992; Smith and Gallacher, 1992). In the currently accepted model, Cl^- is driven into the cytoplasm against its electrochemical gradient via Na^+-K^+-$2Cl^-$ cotransporter (NKCC) and/or via parallel operations of Na^+-H^+ and Cl^--HCO_3^- exchangers, using the energy in the Na^+ gradient across the basolateral membrane that is maintained by the activity of Na^+-K^+ ATPase (Pirani et al., 1987; Lau et al., 1990; Petersen, 1992; Turner, 1993). These transporters raise intracellular Cl^- concentration ($[Cl^-]_i$) to levels (~60 mM) that are significantly greater than the electrochemical equilibrium level (Foskett, 1990), providing a driving force for Cl^- to exit the cell across the apical membrane via a Cl^- channel. The secretory isoform of the Na^+-K^+-$2Cl^-$ cotransporter (NKCC1) was suggested to play a key role in the movement of electrolytes and water across secretory epithelia, and the control of $[Cl^-]_i$ (Soltoff et al., 1989; Evans and Turner, 1997; Russell, 2000). Reduction of $[Cl^-]_i$ resulting from secretory Cl^- loss appears to stimulate NKCC activity, presumably via the cotransporter phosphorylation, whereas elevation of $[Cl^-]_i$ has been shown to inhibit NKCC activity in secretory epithelia (Foskett, 1990; Lytle and Forbush, 1992; Robertson and Foskett, 1994; Haas et al., 1995;

Address correspondence to Makoto Sugita, Department of Oral Physiology, Graduate School of Biomedical Sciences, Hiroshima University, Kasumi 1-2-3, Minami-ku, Hiroshima 734-8553, Japan. Fax: 81-82-257-5627; email: sugisan@hiroshima-u.ac.jp

Abbreviations used in this paper: BCECF, 2',7'-bis(2-carboxyethyl)-5(6)-carboxyfluorescein; CCh, carbachol; DPC, diphenylamine-2-carboxylate; KHR, Krebs-Henseleit Ringer; NHE, Na^+-H^+ exchanger; NKCC, Na^+-K^+-$2Cl^-$ cotransporter; NPPB, 5-nitro-2-(3-phenylpropylamino) benzoic acid.

J. Gen. Physiol. © The Rockefeller University Press • 0022-1295/2004/07/59/11 $8.00
Volume 124 July 2004 59–69
http://www.jgp.org/cgi/doi/10.1085/jgp.200308948

Putney et al., 1999). Thus, regulation of the NKCC by $[Cl^-]_i$ may play a role in mediating cross-talk between the basolaterally located NKCC and apical Cl^- channels in secretory epithelia (Lytle and Forbush, 1992; Robertson and Foskett, 1994). Ca^{2+}-mobilizing agonists also stimulate Na^+-H^+ exchanger (NHE) activity, which promotes both the uptake of Cl^- mediated by a pH_i-coupled basolateral Cl^--HCO_3^- exchanger, and the secretion of HCO_3^- generated via metabolic pathways involving a carbonic anhydrase (Melvin et al., 1988; Lau et al., 1989; Soltoff et al., 1989; Manganel and Turner, 1991; Robertson and Foskett, 1994). Cl^- and HCO_3^- secretion by acinar cells is tightly regulated by $[Ca^{2+}]_i$ and involves changes in the activities of several transport proteins as well as intracellular ion composition and membrane potential. The complexities of the secretory responses in exocrine acinar cells complicate the task of determining the relative contributions and interactions of these various transport pathways and regulatory events. Previous studies that monitored fluid secretion and intracellular pH in intact submandibular glands revealed a dominant involvement of the NKCC activity in controlling the rate of fluid and electrolyte secretion (Martinez and Cassity, 1985; Pirani et al., 1987; Lau et al., 1990). Recent studies of parotid acinar cells from either NHE- or NKCC-deficient mice also indicated that NKCC is the major chloride influx pathway during the early stages of salivation, although the contribution of NHE activity increased during prolonged stimulation (Evans et al., 1999, 2000; Park et al., 2001a). However, the rates of Cl^- secretion were not directly determined in those reports, although the secretion rate was estimated by measuring intracellular pH and the saliva flow rate. Furthermore, the nature of transcellular Cl^- movement in exocrine acinar cells, where the membrane proteins regulating $[Cl^-]_i$ are functionally intact, and $[Cl^-]_i$ serves as a messenger for cross-talk between apical and basolateral membrane proteins, remains elusive at a single cell level. The efficiency of Cl^- secretion will depend upon the level of expression of the relevant transport proteins, the relevant driving forces, and the relative turnover rates of the transport proteins. Since activation of salivary secretion by cholinergic agonists is associated with $[Ca^{2+}]_i$ oscillations, the activity of the Ca^{2+}-activated channels will oscillate, and $[Cl^-]_i$ may fluctuate as well (Foskett and Melvin, 1989). Thus, it is likely that driving forces, transport activities, and regulatory influences may dynamically determine the rate of oscillatory Cl^- secretion.

To characterize the contribution of those activities to the net Cl^- secretion evoked by Ca^{2+} mobilizing agonists in submandibular acinar cells, we employed the gramicidin-perforated patch recording. The linear pentadecapeptide antibiotic gramicidin is a naturally occurring product of *Bacillus bravis* known to form monovalent cation selective channels in synthetic and natural membranes (Mueller and Rudin, 1967; Andersen and Koeppe, 1992). Although the structure of the active gramicidin channel remains a source of controversy, gramicidin creates the pores that are completely impermeable to anions (Burkhart et al., 1998; Kovacs et al., 1999; Allen et al., 2003). In contrast, the antibiotic ionophores nystatin and amphotericin B, which are commonly used for the perforated patch methods, allow permeation of not only monovalent cations but also Cl^-. Thus, the use of gramicidin in the perforated patch technique enables whole-cell electrophysiological analyses to be performed with normal cellular composition of intracellular anions. Cl^- currents measured in gramicidin-perforated patch recordings are dependent upon Cl^- entry through the cohort of transporters expressed in acinar cells. We therefore considered that the gramicidin-perforated patch configuration is a powerful tool for investigating the secretory mechanisms that coordinate activities of basolateral membrane–located Cl^- influx transporters with apical membrane–located Cl^- efflux channels in secretory epithelial cells.

In the present study, the Ca^{2+}-activated Cl^- current in isolated submandibular acinar cells was characterized using the gramicidin-perforated patch configuration, which enabled us to analyze the relative contributions of the different Cl^- influx pathways and the efflux pathway to Cl^- secretion. Carbachol (CCh), a Ca^{2+} mobilizing agonist, evoked oscillatory Cl^- currents that were associated with synchronous oscillations of membrane potential. The pharmacological sensitivities of the current revealed that the oscillatory Cl^- current represents the Cl^- exit via Ca^{2+}-activated Cl^- channels, dependent on Cl^- entry through NKCC. Furthermore, the deduced characteristics of secretory Cl^- movements, governed by the concerted effort of NKCC and the Ca^{2+}-activated Cl^- channel, suggest that the steep control of their transport activities by $[Ca^{2+}]_i$ and $[Cl^-]_i$ may underlie the efficient driving of oscillatory Cl^- secretion in intact submandibular acinar cells.

MATERIALS AND METHODS

Materials

CCh, gramicidin, bumetanide, methazolamide, genistein and 5-nitro-2-(3-phenylpropylamino)benzoic acid (NPPB) were purchased from Sigma-Aldrich. Diphenylamine-2-carboxylate (DPC) was purchased from Wako Pure Chemical. The media used were based on Krebs-Henseleit Ringer (KHR) solution containing 103 mM NaCl, 4.7 mM KCl, 2.56 mM $CaCl_2$, 1.13 mM $MgCl_2$, 25 mM $NaHCO_3$, 1.15 mM NaH_2PO_4, 2.8 mM glucose, 4.9 mM sodium pyruvate, 2.7 mM sodium fumarate, 4.9 mM sodium glutamate, and 0.1% BSA, buffered with 12.5 mM HEPES at pH 7.4. The solution was thoroughly gassed with 95% O_2 and 5% CO_2 before each experiment.

Isolation of Acinar Cells

This study was approved by the Committee of Research Facilities for Laboratory Animal Science, Hiroshima University School of Medicine. The animals were treated in accordance with the Guide for the Care and Use of Laboratory Animals (National Academy of Sciences), and the Guide for Animal Experimentation, Hiroshima University, and extra care was taken to avoid animal suffering. Male Wistar rats (~300 g) were anesthetized by the intraperitoneal injection of sodium pentobarbital (Nembutal, 70 mg/kg). Isolated rat submandibular acinar cells were prepared using collagenase (260 U/ml; type S-1, Nitta Gelatin) digestion as previously described (Sugita et al., 2000). The acinar cells were allowed to stick onto coverslips coated with poly-L-lysine (Sigma-Aldrich).

Gramicidin-perforated Patch Recording from Isolated Acinar Cells

The acinar cells on the cover glass were placed in a 0.2-ml chamber containing the KHR solution connected to a bath electrode by a 150 mM KCl-agar bridge. The chamber was constantly perfused at a rate of 1 ml/min with KHR solution without BSA at room temperature. Patch-clamp pipettes (2–4 MΩ) were pulled from borosilicate glass capillaries (Garner Glass Company). The gramicidin-perforated patch pipette solution contained 150 mM KCl and 10 mM HEPES (adjusted to pH 7.4 with KOH). Gramicidin was first dissolved in methanol to a concentration of 10 mg/ml and then diluted in the pipette solution to a final concentration of 100 μg/ml immediately before use. Before backfilling the pipette with the gramicidin-containing solution, the pipette tip was filled with gramicidin-free pipette solution by a brief immersion. After obtaining a gigaseal, the command potential was set at −40 mV, so that before membrane perforation, the transpatch potential was close to 0 mV, and after perforation, the cell was roughly at resting potential. Gramicidin-perforated patch recording was started after the stabilization of the capacitive currents (~15–25 min after cell attachment) (Ebihara et al., 1995; Sugita et al., 2000). The membrane potential of isolated acinar cells was measured under the current-clamp condition in the gramicidin-perforated patch configuration. Ionic currents were measured under voltage clamping at the holding potential of −80 mV, a value close to the potassium equilibrium potential. In experiments testing the effect of external anions, the perfused solution was modified by replacing 103 mM NaCl with equimolar quantities of the corresponding sodium salt of other anions. Thus, 12 mM Cl^- was still present in the substituted solution. Ionic currents and voltage were measured with a patch/whole-cell clamp amplifier CEZ-2400 (Nihon Kohden), digitized with a MacLab/200 (AD Instruments), and recorded directly onto hard disk (Macintosh Performa 5260) (Hirono et al., 2001). Oscillatory events of Cl^- currents were detected and analyzed using MacLab Chart 3.5 (AD Instruments). The base lines of current traces and the peak current amplitudes were determined by computer-assisted manual detection. As shown in Fig. 3 A, the periods of an increasing phase (T_i) and a decreasing phase (T_d) were derived from duration analysis of the detected events from the inward current traces. The durations spent to reach one half of the peak amplitude in the increasing phase and the decreasing phase was denoted as $T_{i(1/2)}$ and $T_{d(1/2)}$, respectively.

Whole-cell Patch Recording from Isolated Acinar Cells

Conventional whole-cell patch recording was performed as described previously (Hirono et al., 1998). The pipette solution contained 140 mM KCl, 1 mM $MgCl_2$, 10 mM HEPES, 0.5 mM EGTA, 10 mM glucose, and 1 mM ATP (adjusted to pH 7.4 with KOH). To establish whole-cell recording, additional suction was performed to rupture the patch membrane after the gigaseal formation. Chloride and potassium currents of the cells were isolated by changing the membrane potential from the holding potential (−80 mV, a value close to the potassium equilibrium potential) to 0 mV, a value close to the chloride equilibrium potential, briefly (500 ms) at 2-s intervals.

Measurement of Intracellular pH (pH_i) and Determination of NKCC Activity

The isolated acinar cells were loaded with the pH-sensitive indicator, 2',7'-bis(2-carboxyethyl)-5(6)-carboxyfluorescein (BCECF), by incubation in the presence of 2 μM BCECF-AM (Dojindo) for 15 min in the KHR solution containing 0.1% BSA. The cells were attached to the coverslips coated with poly-L-lysine, placed in a 0.5-ml chamber, and constantly perfused at a rate of 5 ml/min with KHR solution without BSA. Intracellular BCECF fluorescence was monitored using an inverted epifluorescence microscope equipped with an image analysis system, ARGUS-HiSCA (Hamamatsu Photonics). Cells were sequentially excited at 490 and 450 nm for 272 ms at 2-s intervals, and the emitted fluorescence images were stored in a computer. After each experiment, cells were perfused with the solution containing 140 mM KCl, 10 mM NaCl, 1 mM $MgSO_4$, 10 mM HEPES, and 5 μM nigericin at various pH values (6.8 ~ 7.8) to monitor the fluorescence for pH_i calibration. Fluorescence ratios (F490/F450) were then calculated and converted to pH_i. The pH_i measurement was performed within 2 h after the cell isolation. During the period, the isolated cells seemed to be healthy, judged by the fact that the Ca^{2+} pumping activity, required for oscillatory Cl^- movement, remained unchanged.

The NKCC activity of isolated acinar cells was measured by determining the initial rate of pH_i recovery from an NH_4Cl-induced acute alkaline load, as described previously (Paulais and Turner, 1992; Evans and Turner, 1997). Following various experimental treatments, the acinar cells were subjected to a 30 mM NH_4Cl challenge. The cells first rapidly alkalinized and then recovered exponentially to a final pH_i. By using the program DeltaGraph PRO3 (DeltaPoint), the recovery traces were fitted to an exponential equation

$$pH_t = (pH_{initial} - pH_{final})e^{-kt} + pH_{final},$$

where pH_t is the value of pH_i at time t, $pH_{initial}$ is the initial alkaline pH_i induced by the addition of NH_4^+ (at $t = 0$), pH_{final} is the final resting pH_i after NH_4^+ addition, and k is the recovery rate constant. The recovery traces were fitted by using least-squares curve-fitting techniques and treating $pH_{initial}$, pH_{final}, and k as free parameters. The initial pH_i recovery rate is given by $k(pH_{initial} - pH_{final})$.

Results are presented as means ± SEM of n observations. Unless noted otherwise, statistical significance was determined using unpaired t test. P values <0.05 were considered statistically significant.

RESULTS

CCh Induces Repetitive Spikes of Cl^- Currents in the Gramicidin-perforated Patch Configuration

First, submandibular acinar cells were voltage clamped in the conventional whole-cell patch configuration and stepped between −80 mV and 0 mV. CCh, a Ca^{2+}-mobilizing agonist, induced repetitive spikes of inward cur-

rent and a sustained increase in outward current (Fig. 1 A). The inward and outward currents were expected to be Ca^{2+}-activated ICl and IK, respectively, as previously reported in rat salivary acinar cells (Hirono et al., 1998). DPC (500 μM), a nonspecific Cl^- channel inhibitor (Poronnik et al., 1992; Zeng et al., 1997), markedly suppressed the oscillatory Cl^- currents induced by CCh without affecting the sustained K^+ currents (unpublished data). In the gramicidin-perforated patch configuration, the membrane potential of isolated acinar cells was measured under the current-clamp conditions, and ionic currents were measured at the holding potential of −80 mV, a value close to the K^+ equilibrium potential. Representative traces of the ionic current and membrane potential, recorded by repetitively switching between the voltage clamp mode and the current clamp mode, are shown in Fig. 1 B. The average current and membrane potential under resting conditions were 0.09 ± 0.01 nA and −45.23 ± 0.88 mV (n = 19), respectively. CCh induced repetitive spikes of inward current that were associated with synchronous oscillations of membrane potential (Fig. 1 C). Although variability in the magnitude and kinetics of the inward current spikes was observed, CCh-triggered repetitive spikes of inward current and membrane potential oscillations had an average frequency of ~0.4 Hz (Fig. 1 C). DPC (500 μM) inhibited the oscillatory inward current and eliminated the membrane potential oscillations, while causing the voltage to hyperpolarize in the direction of the K^+ equilibrium potential ($P < 0.05$, n = 3, paired t test) (Fig. 1 D). Substitution of external Cl^- with gluconate suppressed the CCh-induced inward current spikes (Fig. 1 E), consistent with the inward current being carried by Cl^-, dependent upon the activity of Ca^{2+}-activated Cl^- channels and Cl^- influx into the cell. In intact acinar cells, the Na^+-K^+ ATPase and Ca^{2+}-activated K^+ channels are essential for salivary secretion, and their concerted actions, together with anion channels and transporters, play key roles in determining the rate of Cl^- secretion. However, because the gramicidin-perforated patch configuration allows permeation of monovalent cations, the requirement for K^+ or Na^+-K^+ ATPase activities is abrogated by voltage- and monovalent cation-clamping. In accord, neither the specific K^+ channel blocker, charybdotoxin, nor the Na^+-K^+ ATPase inhibitor, ouabain, suppressed the CCh-induced inward currents (Fig. 1 F). Thus, the anion efflux rate, measured as the inward current, is determined solely by the activities of anion channels and transporters in the gramicidin-perforated patch configuration. Therefore, the gramicidin-perforated patch recording could enable dissection of the mechanisms specifically involved in mediating Cl^- transport across the apical and basolateral membranes. We have therefore characterized the sustained oscillatory anion currents under different conditions. The responses during the initial 2 min after the addition of CCh were excluded from the quantitative analysis below, since CCh may activate the anion channels possessing the distinct properties in the initial phase and the late phase of fluid secretion (Sugita et al. 2000), and CCh also induces nonoscillatory anion currents during the initial phase.

The Effect of Bumetanide and Methazolamide on the CCh-induced Cl^- Current in the Gramicidin-perforated Patch Configuration

Since gramicidin creates monovalent cation-selective pores, the CCh-activated Cl^- current in the gramicidin-perforated patch recording represents the Cl^- exit via Cl^- channels, dependent on Cl^- entry through membrane proteins expressed in the cells. Thus, to maintain the sustained Cl^- currents in the gramicidin-perforated patch configuration, $[Cl^-]_i$ must be maintained in the cytoplasm above its electrochemical equilibrium value (Fig. 1 G). In the currently accepted model, Cl^- was suggested to enter the cytoplasm against its electrochemical gradient via a loop diuretic-sensitive NKCC and/or via parallel operations of Cl^--HCO_3^- and Na^+-H^+ exchangers (Pirani et al., 1987; Turner and George, 1988; Moore et al., 1995; He et al., 1997). In the gramicidin-perforated patch recording, the loop diuretic bumetanide (500 μM) reduced the CCh-activated Cl^-current by 87.8 ± 10.1% ($P < 0.05$, n = 4) (Fig. 2, A and B), and caused the membrane potential to hyperpolarize in the direction of the K^+ equilibrium potential ($P < 0.05$) (Fig. 2, A and B). To inhibit Cl^--HCO_3^- exchange activity, we employed methazolamide, a carbonic anhydrase inhibitor, to minimize the amount of HCO_3^- available in the cytoplasm for transport. The previous study using parotid duct cells indicated that methazolamide suppressed the forskolin-activated anion current in the gramicidin-perforated patch configuration (Hirono et al., 2001). Although the addition of methazolamide (500 μM) after bumetanide application sometimes caused a slight inhibition of the CCh-activated Cl^- current (Fig. 2, A and B), there was no statistical difference between the currents in the experimental conditions of CCh + bumetanide, and CCh + bumetanide + methazolamide. Methazolamide alone had little effect on the CCh-activated Cl^- current or membrane potential oscillations (Fig. 2, C and D). In contrast, addition of bumetanide after methazolamide application markedly reduced the CCh-activated Cl^- current by 97.7 ± 3.5% ($P < 0.05$, n = 3) (Fig. 2, C and D), and caused the membrane potential to hyperpolarize in the direction of the K^+ equilibrium potential ($P < 0.05$) (Fig. 2, C and D). Neither methazolamide nor bumetanide had significant effects on the frequencies of the current spikes (Fig. 2 G). Importantly, in the conventional

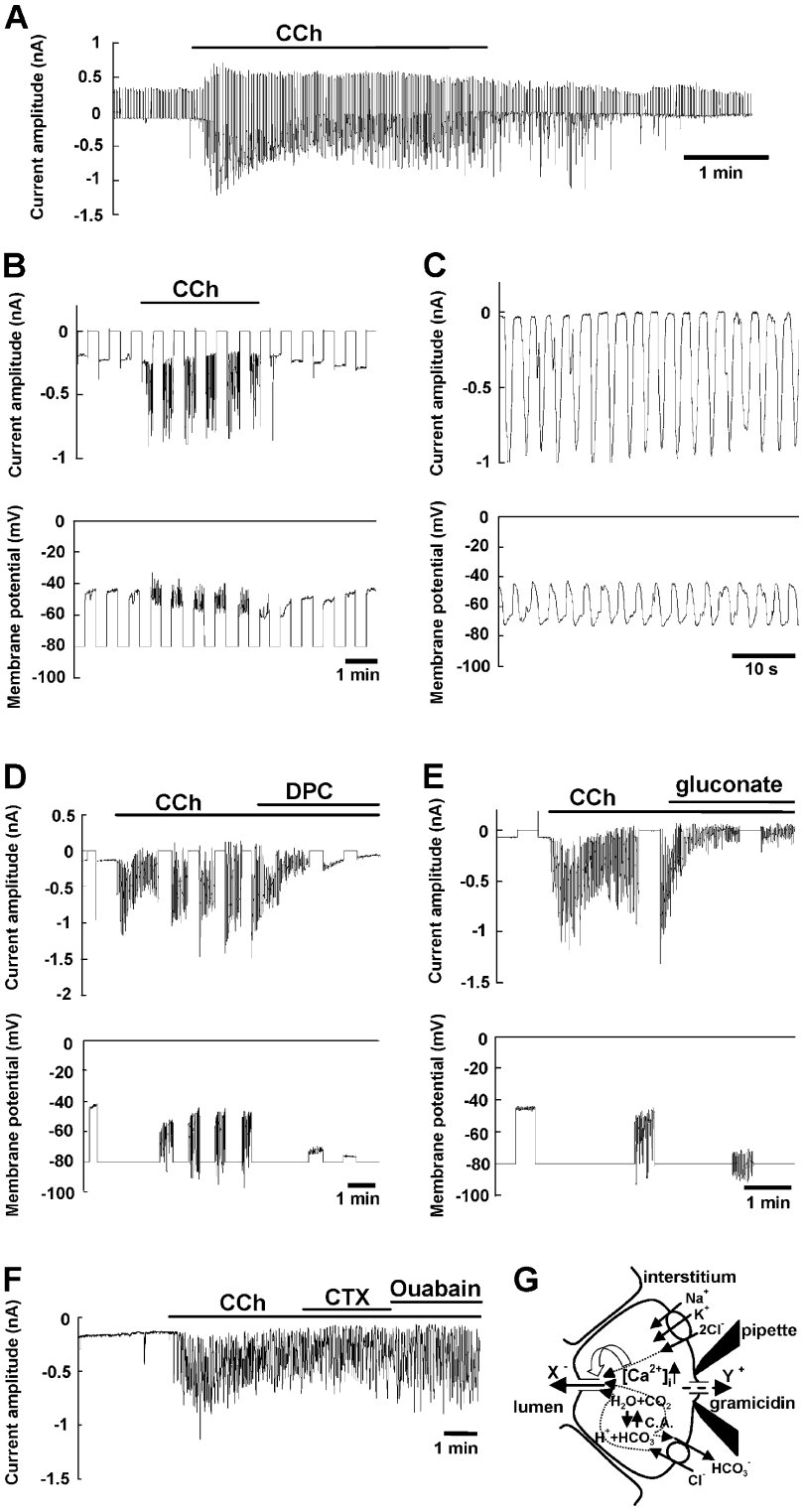

FIGURE 1. CCh induces repetitive spikes of Cl^- currents associated with the oscillations of membrane potential. (A) CCh-induced Cl^- and K^+ currents in the conventional whole-cell patch configuration were measured in submandibular acinar cells that were voltage clamped and stepped between −80 mV and 0 mV. CCh (500 nM) was added to the perfusate during the period indicated by the horizontal bar. (B) CCh-induced anion current and changes in membrane potential, recorded in the gramicidin-perforated patch configuration. The current and membrane potential were recorded under the voltage- and current-clamp modes, respectively. Thus, by repetitively switching those modes, the current and membrane potential were measured during the period indicated as −80 mV and 0 nA, respectively. CCh (500 nM) was added to the perfusate during the period indicated by the horizontal bar. (C) Representative time-resolved traces of CCh-induced repetitive spikes of inward current associated with the oscillations of membrane potential. (D) The effects of DPC on CCh-induced inward current and changes in membrane potential. CCh (500 nM) and DPC (500 μM) were added to the perfusate during the period indicated by the horizontal bars. (E) Representative traces of the anion current and membrane potential of isolated acinar cells during the application of CCh with the gluconate substitution. CCh (500 nM) was added to the perfusate, and 103 mM Cl^- in the extracellular solution was replaced by equimolar amounts of gluconate during the period indicated by the horizontal bars. (F) The effects of charybdotoxin and ouabain on the CCh-induced inward current in the gramicidin-perforated patch recording. CCh (500 nM), charybdotoxin (CTX, 100 nM), and ouabain (500 μM) were added to the perfusate during the period indicated by the horizontal bars. (G) Schematic illustration of acinar cells under the gramicidin-perforated patch configuration. The CCh-activated anion currents in the gramicidin-perforated patch recording are dependent on the Cl^- entry transporters, or the production of HCO_3^-. The currently accepted model of the distribution of key anion transport proteins in submandibular acinar cells is also shown. Depicted in the apical membrane is the Ca^{2+}-activated anion channel(s). Depicted in the basolateral membrane are a Na^+-K^+-$2Cl^-$ cotransporter and a Cl^--HCO_3^- exchanger. Also shown is CO_2 diffusing across the basolateral membrane and reacting with H_2O in the presence of carbonic anhydrase (C.A.) to form H^+ and HCO_3^-.

whole-cell patch configuration, neither bumetanide nor methazolamide affected the CCh-induced repetitive spikes of inward current or the sustained increase in outward current, expected to be Ca^{2+}-activated *I*Cl and *I*K, respectively. In a different protocol, external HCO_3^- (25 mM) was completely eliminated in the gramicidin-perforated patch configuration. The absence of HCO_3^- was without effect on the CCh-induced inward current (Fig. 2 F). Thus, the present results suggest that Cl^--HCO_3^- exchange activity does not contribute significantly to the Cl^- uptake that maintains sustained Cl^- efflux currents. The use of

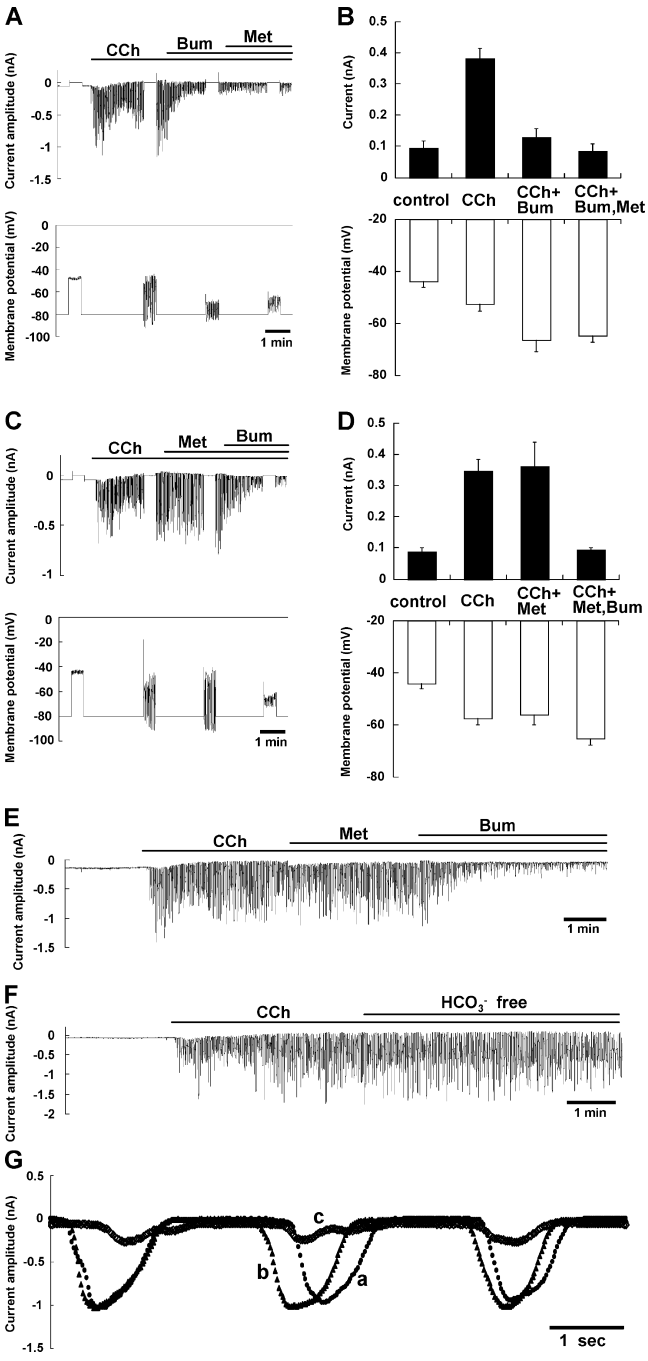

FIGURE 2. The effects of bumetanide and methazolamide on the CCh-induced anion current and oscillations of membrane potential in the gramicidin-perforated patch configuration. (A and C) Representative traces of the anion current and membrane potential of isolated acinar cells during the application of CCh (500 nM), bumetanide (Bum, 500 μM), and methazolamide (Met, 500 μM) added to the perfusate during the period indicated by the horizontal bars. (B and D) Comparison of the CCh-induced anion current and the average membrane potential in the presence of bumetanide and/or methazolamide. The average current and membrane potential in B and D were determined in the final 20 s before switching between the voltage and current clamp modes in the absence (control) or presence of CCh, followed by the sequential addition of bumetanide and/or methazolamide, as indicated in A and C, respectively (n = 3–5). (E) The effects of the addition of Na^+ to the pipette on the CCh-induced anion current. The CCh-induced anion current was recorded using the pipette solution containing 145 mM KCl, 5 mM NaCl, and 10 mM HEPES (pH 7.4), and the effects of bumetanide (500 μM) and methazolamide (500 μM) on the current were determined. (F) The effect of the external HCO_3^- depletion on the CCh-induced anion current. CCh (500 nM) and the HCO_3^--free external solution, in which 25 mM HCO_3^- was replaced by Cl^- and CO_2 was removed, were applied during the period indicated by the horizontal bars. (G) The representative time-resolved traces of the CCh-induced repetitive spikes of inward current in the presence of methazolamide and bumetanide. The traces of the CCh-induced inward currents before (a, closed circles) and after (b, closed triangles) the application of methazolamide, followed by the simultaneous addition of methazolamide and bumetanide (c, open diamonds), were deduced from a single gramicidin-perforated patch recording.

Na^+-free solutions in the pipette in the perforated patch configuration increased the inward driving force for Cl^- uptake on both the cotransporter and the paired exchangers, compared with the normal in vivo conditions. However, addition of 5 mM Na^+ to the pipette had little effect on the amplitude of the CCh-induced anion current or its sensitivities to methazolamide and bumetanide (Fig. 2 E). Taken together, these results indicate that NKCC activity is the predominant mediator of Cl^- influx across the basolateral membrane of submandibular acinar cells under the experimental conditions used, as well as when the physiological intracellular and extracellular concentrations of Na^+, K^+, and Cl^- are maintained.

To evaluate if NKCC activity limits the magnitude of the CCh-activated Cl^- current, we compared the duration elements of the oscillatory spikes of CCh-induced inward currents (Fig. 3, A and B). Bumetanide, but not methazolamide, significantly decreased $T_{d(1/2)}$ and T_d ($P < 0.05$) (Fig. 3 B), without effect on $T_{d(1/2)}/T_d$. Neither $T_{i(1/2)}$ nor T_i was affected by the application of either drug. These results indicate that the duration of a decreasing phase of the current spikes may be prolonged by the NKCC activity, possibly by supplying sufficient Cl^- to the channel efflux pathway.

The Effects of the Modifier of NKCC Activity on the CCh-induced Cl^- Currents

The gramicidin-perforated patch configuration allows us to evaluate the electroneutral transport of ions by NKCC, which was not detectable in the conventional electrophysiological measurements. The loop diuretic sensitivity of the CCh-activated Cl^- current and membrane potential oscillations suggests that, by comparison with the paired exchangers, NKCC is the dominant Cl^- influx pathway for supporting the oscillatory Cl^- efflux through the Cl^- channels in submandibular acinar cells. Next, we addressed the contributory role of the activity of the Ca^{2+}-activated Cl^- efflux channel and the

Cl^- influx activity via the cotransporter in the transcellular Cl^- movement. To characterize the involvement of the NKCC activity in determining the amplitude of oscillatory Cl^- currents, we investigated the effects of reagents that modify cotransporter activity. Genistein, a flavonoid contained in soybean and other various foods, was reported to stimulate Cl^- transport in epithelial tissues through the activation of cystic fibrosis transmembrane conductance regulator, an epithelial Cl^- channel, and NKCC (Wang et al., 1998; Niisato et al., 1999). To determine if genistein stimulates Na^+-K^+-$2Cl^-$ transport in submandibular acinar cells, we analyzed NKCC activity by determining the rate of pH_i recovery of cells from an NH_4Cl-induced alkaline load, as previously described (Paulais and Turner, 1992; Evans and Turner, 1997). Application of CCh, before an NH_4Cl-induced alkaline load, induced the cytosolic acidification created by the initial HCO_3^- efflux. The recovery from the acid load, previously reported in salivary acinar cells, was not clearly observed in our experiments. The different response may be derived from the difference in the CCh dose used in the experiments, and the resultant differences in elevations of $[Ca^{2+}]_i$ and the activities of NHEs and the other ion transporters. Of note, the dose-dependent changes in the pH_i of submandibular glands in the HCO_3^--containing medium was previously reported as stimulation with a submaximal concentration of acetylcholine caused a fall in pH_i in sharp contrast to the effect of a maximal concentration (Pirani et al., 1987). The initial rate of pH_i recovery from an NH_4Cl-induced alkaline load, calculated from the pH_i traces of the CCh-preincubated acinar cells in the presence of external HCO_3^-, was 0.43 ± 0.03 pH U/min (n = 27) (Fig. 4, A and C). The initial pH_i recovery from the alkaline load was markedly slowed by bumetanide (0.12 ± 0.01 pH U/min, $P < 0.05$; n = 11) (Fig. 4, A and C). Genistein (100 μM) accelerated the initial rate of pH_i recovery of the CCh-preincubated acinar cells (0.59 ± 0.04 pH U/min, $P < 0.05$; n = 14) (Fig. 4, B and C). The genistein-stimulated recovery was inhibited by bumetanide to a rate of 0.10 ± 0.01 pH U/min (Fig. 4, B and C), suggesting that it stimulated NKCC activity. In the conventional whole-cell patch configuration, the addition of genistein had little effect on the CCh-induced repetitive spikes of inward current and sustained increase in outward current, expected to be Ca^{2+}-activated ICl and IK, respectively (Fig. 4, D and F). In contrast, genistein significantly increased the CCh-induced Cl^- current in the gramicidin-perforated patch configuration ($P < 0.05$; n = 3, paired t test) (Fig. 4, E and F). The genistein-induced enhancement was sensitive to bumetanide (Fig. 4 E). Thus, genistein enhanced CCh-induced Cl^- currents indirectly, by enhancing NKCC activity without affecting the activity of Ca^{2+}-activated Cl^- channels directly.

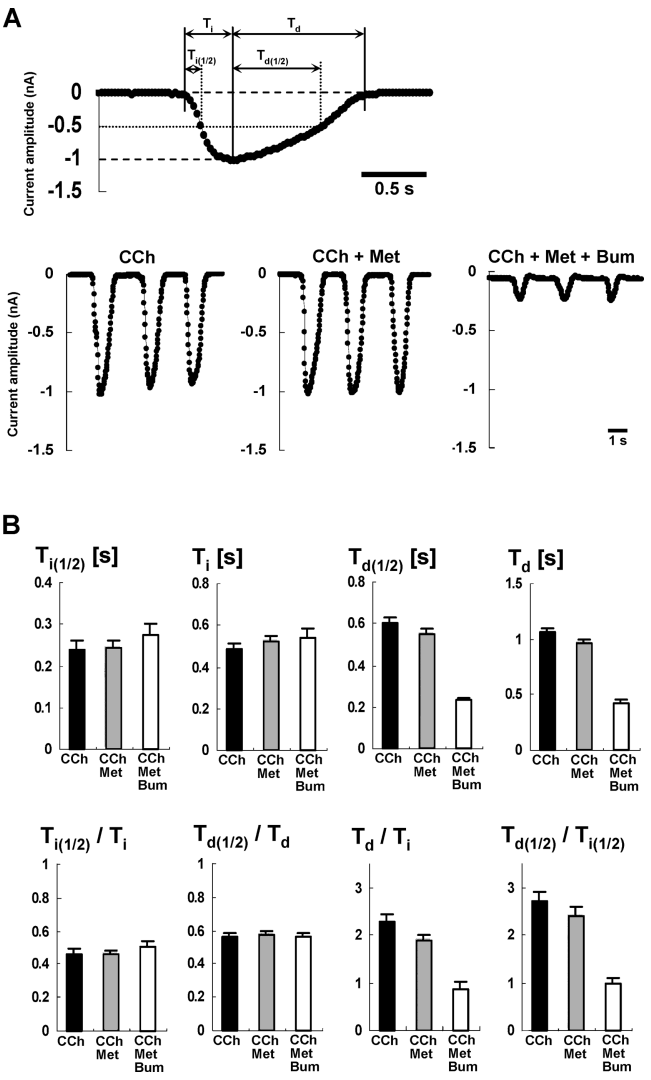

FIGURE 3. Comparison of the durations of the oscillatory spikes of CCh-induced inward currents in the presence or absence of bumetanide and methazolamide. (A) Schematic representation of the analyzed durations in the CCh-induced inward currents (in the top panel). The periods of an increasing phase (T_i) and a decreasing phase (T_d) were determined in the various experimental procedures. Also, the durations spent to reach one half of the peak amplitude in the increasing phase ($T_{i(1/2)}$) and the decreasing phase ($T_{d(1/2)}$) were calculated. The lower panels show the representative traces employed to analyze the oscillatory events of the CCh-induced inward current before and after the application of methazolamide (500 μM), followed by the simultaneous addition of methazolamide and bumetanide (500 μM). (B) Comparison of $T_{i(1/2)}$, T_i, $T_{d(1/2)}$, T_d, $T_{i(1/2)}/T_i$, $T_{d(1/2)}/T_d$, T_d/T_i, and $T_{d(1/2)}/T_{i(1/2)}$ in the CCh-induced repetitive spikes of inward currents from the isolated acinar cells in the presence or absence of methazolamide and bumetanide. Results are presented as means ± SEM (n = 11).

The Effect of NPPB on the CCh-induced Cl^- Currents

To further characterize the relative contributions of the activities of NKCC and the Ca^{2+}-activated Cl^- channel to transcellular Cl^- movement, we took the converse approach of partially inhibiting the channel activity. We

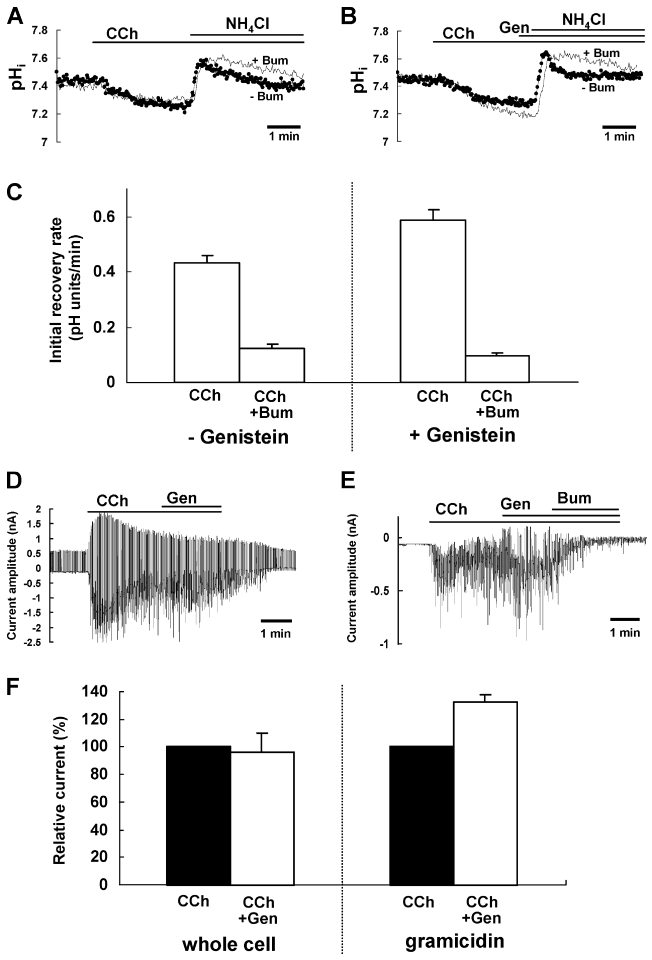

FIGURE 4. Effect of genistein on NKCC activity and the CCh-induced Cl^- currents. (A) Representative pH_i traces from isolated acinar cells challenged with NH_4Cl. CCh (500 nM) and NH_4Cl (30 mM) were added to the perfusate during the period indicated by the horizontal bars. The traces were from the acinar cells with (the thin line) or without (closed circles) bumetanide (Bum, 500 μM) added 20 s before the application of NH_4Cl. (B) Representative pH_i traces from isolated acinar cells preincubated with genistein and challenged with 30 mM NH_4Cl. CCh (500 nM), genistein (Gen, 100 μM), and NH_4Cl (30 mM) were added to the perfusate during the period indicated by the horizontal bars. The traces were from the acinar cells with (the thin line) or without (closed circles) bumetanide (500 μM) added 20 s before the application of NH_4Cl. (C) Comparison of the initial rates of pH_i recovery from an NH_4^+-induced alkaline load, determined in CCh-pretreated acinar cells in the presence or absence of genistein. The initial recovery rates were calculated from pH_i traces indicated as A and B, as described in MATERIALS AND METHODS. Results are presented as means ± SEM of the initial recovery rates from CCh-pretreated cells ($n = 27$), CCh- and Bum-pretreated cells ($n = 8$), CCh- and Gen-pretreated cells ($n = 14$), and CCh-, Gen-, and Bum-pretreated cells ($n = 9$). (D) The effect of genistein on the CCh-induced Cl^- and K^+ currents in the conventional whole-cell patch configuration. (E) The effect of genistein on the CCh-induced anion current recorded under the gramicidin-perforated patch configuration. CCh (500 nM), genistein (Gen, 100 μM), and bumetanide (Bum, 500 μM) were added to the perfusate during the period indicated by the horizontal bars. (F) Comparison of the effect of genistein on the CCh-induced anion currents under either the conventional whole-cell patch or the gramicidin-perforated patch configurations. The relative currents before (black columns) and after (white columns) the addition of genistein were determined in the final 20 s before changing solutions. The relative currents are expressed as a percentage of the anion current induced by CCh alone under either the conventional whole-cell patch or the gramicidin-perforated patch configurations ($n = 3$).

compared the sensitivities of the CCh-induced Cl^- currents to the various concentrations of NPPB, a Cl^- channel blocker, under either the conventional whole-cell or gramicidin-perforated patch configurations. Here, if the NKCC activity predominantly restricts the amplitude of oscillatory Cl^- currents measured in the gramicidin-perforated patch configuration, we expect Cl^- currents in this configuration to be less sensitive to Cl^- channel inhibition than those observed in the whole-cell mode. In agreement with this prediction, 4 μM NPPB had little effect on the Cl^- current measured in the gramicidin-perforated patch configuration (Fig. 5, B and C), whereas it inhibited the conventional whole-cell current by 43.6 ± 4.7% ($P < 0.05$; $n = 3$) (Fig. 5, A and C). These data suggest that partial block of the Cl^- channel did not significantly alter the CCh-activated Cl^- current under the gramicidin-perforated patch configuration. Together, these results suggest that NKCC activity may prevailingly determine the amplitude of the oscillatory Cl^- currents, while adjusting to the rate imposed by the Cl^- channel, in the gramicidin-perforated patch configuration.

DISCUSSION

The present results suggest that gramicidin-perforated patch recording enables direct evaluation of the contributions of both channels and transporters to the Ca^{2+}-activated anion current in single exocrine acinar cells. Under the gramicidin-perforated patch configuration, the CCh-evoked repetitive spikes of inward current were associated with synchronous oscillations in membrane potential. The sensitivity of the current to DPC and gluconate substitution suggests that the CCh-induced spikes of the inward current were mainly carried by Cl^-. Submandibular acinar cells express at least five distinct Cl^- channels; ClC0-like, volume sensitive, inward rectifying, Ca^{2+}-activated, and CFTR-like Cl^- channels (Zeng et al., 1997). The oscillatory nature of the CCh-induced current suggests that the Ca^{2+}-activated Cl^- channel is the dominant Cl^- efflux pathway, tightly regulated by the $[Ca^{2+}]_i$ oscillations, presumably with only minor contributions of other channels to the CCh-induced inward current. In the currently accepted model of the roles of key membrane transport proteins in rat salivary acinar cells, activities of both NKCC and parallel opera-

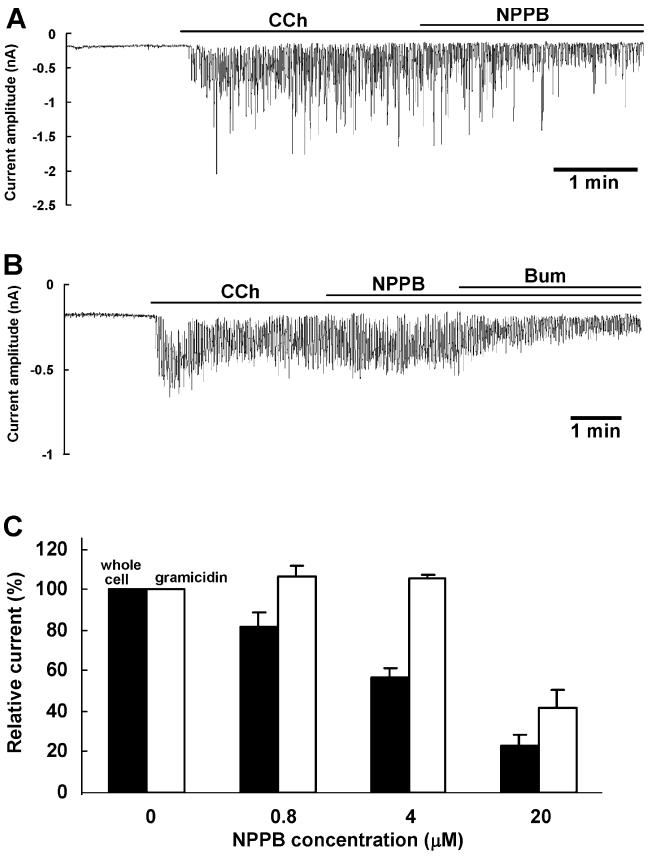

FIGURE 5. Effect of NPPB on the CCh-induced Cl^- currents. (A) Representative trace showing the effect of 4 μM NPPB on the CCh-induced Cl^- current in the conventional whole-cell patch configuration. (B) Representative trace showing the effect of 4 μM NPPB on the CCh-induced anion current recorded under the gramicidin-perforated patch configuration. CCh (500 nM), NPPB (4 μM), and bumetanide (Bum, 500 μM) were added to the perfusate during the period indicated by the horizontal bars. (C) Comparison of NPPB sensitivity of the CCh-induced anion currents under either the conventional whole-cell patch (black columns) or the gramicidin-perforated patch configurations (white columns). The relative currents after the addition of the various concentrations of NPPB were determined from the current traces as shown in A and B. The relative currents are expressed as a percentage of the anion current induced by CCh alone under either the conventional whole-cell patch or the gramicidin-perforated patch configurations ($n = 3$ or 4).

tions of Cl^--HCO_3^- and Na^+-H^+ exchangers were proposed to mediate Cl^- uptake (He et al., 1997; Evans and Turner, 1997; Robertson et al., 1997) although Cl^- uptake by NKCC might dominate over Cl^--HCO_3^- exchange (Pirani et al., 1987; Lau et al., 1990). In parotid acinar cells from either NHE- or NKCC1-deficient mice, Na^+-K^+-$2Cl^-$ cotransport was shown to be the dominant Cl^- uptake mechanism driving fluid secretion during the initial phases of secretion, whereas Cl^--HCO_3^- exchange contributed more to Cl^- influx during sustained muscarinic stimulation, as intracellular pH increased because of enhanced NHE activity (Evans et al., 1999; Evans et al., 2000; Park et al., 2001a). In contrast with the previous reports in which the Cl^- uptake was estimated by monitoring intracellular pH (Pirani et al., 1987; Evans et al., 1999; Park et al., 2001a), our data directly revealed the contribution of transporters to both Cl^- uptake and Cl^- secretion under the gramicidin-perforated patch configuration. As revealed by the effects of bumetanide and methazolamide in the present study, Cl^- uptake was mainly (>85%) mediated by NKCC activity. Interestingly, submandibular acinar cells express at least 10-fold more NKCC protein than do parotid acinar cells (Zeng et al., 1997), which may suggest that the predominant role in submandibular gland cells is accounted for by the higher expression level. HCO_3^- uptake by Na^+-HCO_3^- cotransporters has been proposed in submandibular acinar cells (Luo et al., 2001). However, the contribution of Na^+-HCO_3^- cotransporter activity to the anion currents observed in the present study would seem to be minor, since the elimination of external HCO_3^- had little effect on the CCh-induced anion current under the gramicidin-perforated patch configuration, and the current was remarkably inhibited by bumetanide.

Thus, maintenance of $[Cl^-]_i$ above electrochemical equilibrium appears to be mediated mainly by NKCC, which provides the driving force for Cl^- to exit the cell via a Cl^- channel presumably on the apical membrane. Although the current oscillations appear to reflect the opening and closing of the Cl^- channels tightly regulated by $[Ca^{2+}]_i$ oscillations, which activity, the Ca^{2+}-activated Cl^- channel or the cotransporter, predominantly determines the amplitude of the oscillatory Cl^- currents? To address this issue, first, we investigated the effects of genistein. We found that genistein enhanced the activity of the cotransporter, but was without effect on the activity of the Ca^{2+}-activated Cl^- channel. Nevertheless, genistein stimulated the Cl^- currents in the gramicidin-perforated patch configuration. This result therefore suggests that the activity of the cotransporter is substantially involved in determining the amplitude of the oscillatory Cl^- currents. A similar conclusion was reached in experiments that manipulated the activity of the channel. Thus, partial inhibition of the channel activity by NPPB had much less effect on the CCh-induced Cl^- current under the gramicidin-perforated patch configuration than it did on the Cl^- currents measured in the normal whole-cell configuration. The lower sensitivity implies that the channel activity may not prevailingly determine the rate of current flow in the gramicidin-perforated patch configuration. Finally, our results suggest that the NKCC activity modulated the duration of a decreasing phase of the current spikes. Ca^{2+}-activated Cl^- channels are reported to be regulated by $[Ca^{2+}]_i$ and membrane potential (Arreola et al., 1996; Ishikawa, 1996; Park et al., 2001b). Since the current was recorded

under the voltage-clamp condition, the magnitude of the current reflects the combined influences of $[Ca^{2+}]_i$ and Cl^- driving force. The rate of decay of the Cl^- current following a Ca^{2+} oscillation will reflect the rate of decline of $[Ca^{2+}]_i$ modified by any changes in Cl^- driving force. The observed modulation of the rate of decay of the Cl^- current by bumetanide implies that the rate of Cl^- influx via the cotransporter was involved in determining the amplitude of oscillatory Cl^- currents under this condition as well. Taken together, these results suggest that basolateral NKCC, rather than luminal Ca^{2+}-activated Cl^- channels, may play a prevailing role in restricting the transcellular Cl^- movement induced by CCh in the gramicidin-perforated patch configuration, while the opening and a part of the closing of Ca^{2+}-activated Cl^- channels may participate in restricting the repetitive spikes of Cl^- efflux. The molecular aspects underlying NKCC regulation in exocrine acinar cells remain to be determined (Kurihara et al., 2002). However, it was reported that a reduction of $[Cl^-]_i$, resulting from Cl^- loss through the activated Cl^- channels, reduces $[Cl^-]_i$-mediated inhibition of NKCC (Foskett, 1990; Robertson and Foskett, 1994), presumably by permitting an increase in phosphorylation of NKCC by a Cl^--dependent kinase, and plays a key role in leading to the activation or up-regulation of NKCC (Lytle and Forbush, 1992; Haas et al., 1995; Lytle, 1997; Haas and Forbush, 2000; Flemmer et al., 2002; Dowd and Forbush, 2003). Thus, NKCC appears to be regulated by intracellular Cl^-, allowing the transporter to adjust to the rate imposed by the Cl^- channel. The coordinated activation and inactivation of these transporters may efficiently elicit the oscillatory Cl^- secretion, depending upon $[Ca^{2+}]_i$ and $[Cl^-]_i$. Therefore, it is likely that the manipulation of the NKCC activity has therapeutic value for xerostomia as considered previously (Turner and Sugiya, 2002), since the transcellular Cl^- movement may play an essential role in fluid secretion. Along these lines, genistein might be also be of benefit, particularly in cystic fibrosis by means of up-regulation of NKCC in addition to enhancing the channel activity of the disease-associated CFTR mutants (Wang et al., 1998).

The gramicidin-perforated patch technique is a useful tool for deducing and clarifying the cellular mechanisms underlying ion transport by the concerted effort of the anion efflux channels and the anion influx transporters at a single cell level. Of note, the gramicidin-perforated patch configuration enables the time-resolved determination of the activities of the electroneutral transporters in the cellular systems of ion transport. In the present study, using the CCh-stimulated acinar cells under this configuration, we deduced and characterized the oscillatory nature of secretory Cl^- movements, governed by the Cl^- efflux through the Ca^{2+}-activated Cl^- channels and the Cl^- influx through the electroneutral NKCC, and steeply controlled by $[Ca^{2+}]_i$ and $[Cl^-]_i$. In intact acinar cells, the oscillatory Cl^- movements may effectively drive the oscillatory secretion of fluid and electrolyte, while cooperating with and being regulated by the activities of the Na^+-K^+ ATPase and Ca^{2+}-activated K^+ channels.

We thank Dr. K. Foskett for his critical reading of the manuscript, helpful comments, and his editing for English usage.

This research was supported by a Grant-in-Aid for Scientific Research from the Ministry of Education, Science, Sports, and Culture of Japan (11771137 and 13771094 to M. Sugita).

Olaf S. Andersen served as editor.

Submitted: 19 September 2003
Accepted: 24 May 2004

REFERENCES

Allen, T.W., O.S. Andersen, and B. Roux. 2003. Structure of gramicidin A in a lipid bilayer environment determined using molecular dynamics simulations and solid-state NMR data. *J. Am. Chem. Soc.* 125:9868–9877.

Andersen, O.S., and R.E. Koeppe. 1992. Molecular determinants of channel function. *Physiol. Rev.* 72:S89–S158.

Arreola, J., J.E. Melvin, and T. Begenisich. 1996. Activation of calcium-dependent chloride channels in rat parotid acinar cells. *J. Gen. Physiol.* 108:35–47.

Burkhart, B.M., N. Li, D.A. Langs, W.A. Pangborn, and W.L. Duax. 1998. The conducting form of gramicidin A is a right-handed double-stranded double helix. *Proc. Natl. Acad. Sci. USA*. 95: 12950–12955.

Dowd, B.F., and B. Forbush. 2003. PASK (proline-alanine-rich STE20-related kinase), a regulatory kinase of the Na-K-Cl cotransporter (NKCC1). *J. Biol. Chem.* 278:27347–27353.

Ebihara, S., K. Shirato, N. Harata, and N. Akaike. 1995. Gramicidin-perforated patch recording: GABA response in mammalian neurons with intact intracellular chloride. *J. Physiol.* 484:77–86.

Evans, R.L., and R.J. Turner. 1997. Upregulation of Na^+-K^+-$2Cl^-$ cotransporter activity in rat parotid acinar cells by muscarinic stimulation. *J. Physiol.* 499:351–359.

Evans, R.L., S.M. Bell, P.J. Schultheis, G.E. Shull, and J.E. Melvin. 1999. Targeted disruption of the Nhe1 gene prevents muscarinic agonist-induced up-regulation of Na^+/H^+ exchange in mouse parotid acinar cells. *J. Biol. Chem.* 274:29025–29030.

Evans, R.L., K. Park, R.J. Turner, G.E. Watson, H.-V. Nguyen, M.R. Dennet, A.R. Hand, M. Flagella, G.E. Shull, and J.E. Melvin. 2000. Severe impairment of salivation in $Na^+/K^+/2Cl^-$ cotransporter (NKCC1)-deficient mice. *J. Biol. Chem.* 275:26720–26726.

Flemmer, A.W., I. Gimenez, B.F. Dowd, R.B. Darman, and B. Forbush. 2002. Activation of the Na-K-Cl cotransporter NKCC1 detected with a phospho-specific antibody. *J. Biol. Chem.* 277:37551–37558.

Foskett, J.K. 1990. $[Ca^{2+}]_i$ modulation of Cl^- content controls cell volume in single salivary acinar cells during fluid secretion. *Am. J. Physiol.* 259:C998–C1004.

Foskett, J.K., and J.E. Melvin. 1989. Activation of salivary secretion: coupling of cell volume and $[Ca^{2+}]_i$ in single cells. *Science.* 244: 1582–1585.

Gray, P.T.A. 1988. Oscillations of free cytosolic calcium evoked by cholinergic and catecholaminergic agonists in rat parotid acinar cells. *J. Physiol.* 406:35–53.

Haas, M., and B. Forbush. 2000. The Na-K-Cl cotransporter of secretory epithelia. *Annu. Rev. Physiol.* 62:515–534.

Haas, M., D. McBrayerm, and C. Lyte. 1995. $[Cl^-]_i$-dependent phosphorylation of the Na-K-Cl cotransport protein of dog tracheal epithelial cells. *J. Biol. Chem.* 270:28955–28961.

He, X., C.M. Tse, M. Donowitz, S.L. Alper, S.E. Gabriel, and B.J. Baum. 1997. Polarized distribution of key membrane transport proteins in the rat submandibular gland. *Pflugers Arch.* 433:260–268.

Hirono, C., M. Sugita, K. Furuya, S. Yamagishi, and Y. Shiba. 1998. Potentiation by isoproterenol on carbachol-induced K^+ and Cl^- currents and fluid secretion in rat parotid. *J. Membr. Biol.* 164: 197–203.

Hirono, C., T. Nakamoto, M. Sugita, Y. Iwasa, Y. Akagawa, and Y. Shiba. 2001. Gramicidin-perforated patch analysis on HCO_3^- secretion through a forskolin-activated anion channel in rat parotid intralobular duct cells. *J. Membr. Biol.* 180:11–19.

Ishikawa, T. 1996. A bicarbonate- and week acid-permeable chloride conductance controlled by cytosolic Ca^{2+} and ATP in rat submandibular acinar cells. *J. Membr. Biol.* 153:147–159.

Kovacs, F., J. Quine, and T.A. Cross. 1999. Validation of the single-stranded channel conformation of gramicidin A by solid-state NMR. *Proc. Natl. Acad. Sci. USA.* 96:7910–7915.

Kurihara, K., N. Nakanishi, M.L. Moore-Hoon, and R.J. Turner. 2002. Phosphorylation of the salivary Na^+-K^+-$2Cl^-$ cotransporter. *Am. J. Physiol. Cell Physiol.* 282:C817–C823.

Lau, K.R., A.C. Elliot, and P.D. Brown. 1989. Acetylcholine-induced intracellular acidosis in rabbit salivary gland acinar cells. *Am. J. Physiol.* 256:C288–C295.

Lau, K.R., A.J. Howorth, and R.M. Case. 1990. The effects of bumetanide, amiloride, and Ba^{2+} on fluid and electrolyte secretion in rabbit salivary gland. *J. Physiol.* 425:407–427.

Lee, M.G., X. Xu, W. Zeng, J. Diaz, T.H. Kuo, F. Wuytack, L. Racymaekers, and S. Muallem. 1997a. Polarized expression of Ca^{2+} pumps in pancreatic and salivary gland cells. Role in initiation and propagation of $[Ca^{2+}]_i$ waves. *J. Biol. Chem.* 272:15771–15776.

Lee, M.G., X. Xu, W. Zeng, J. Diaz, R.J. Wojcikiewicz, T.H. Kuo, F. Wuytack, L. Racymaekers, and S. Muallem. 1997b. Polarized expression of Ca^{2+} channels in pancreatic and salivary gland cells. Correlation with initiation and propagation of $[Ca^{2+}]_i$ waves. *J. Biol. Chem.* 272:15765–15770.

Luo, X., J.Y. Choi, S.B.H. Ko, A. Pushkin, I. Kurtz, W. Ahn, M.G. Lee, and S. Muallem. 2001. HCO_3^- salvage mechanisms in the submandibular gland acinar and duct cells. *J. Biol. Chem.* 276: 9808–9816.

Lytle, C. 1997. Activation of the avian erythrocyte Na-K-Cl cotransport protein by cell shrinkage, cAMP, fluoride, and calyculin-A involves phosphorylation at common sites. *J. Biol. Chem.* 272: 15069–15077.

Lytle, C., and B. Forbush. 1992. The Na-K-Cl cotransport protein of shark rectal gland. II. Regulation by direct phosphorylation. *J. Biol. Chem.* 267:25438–25443.

Manganel, M., and R.J. Turner. 1991. Rapid secretagogue-induced activation of Na^+/H^+ exchange in rat parotid acinar cells. *J. Biol. Chem.* 266:10182–10188.

Martinez, J.R., and N. Cassity. 1985. Cl^- requirement for saliva secretion in the isolated, perfused rat submandibular gland. *Am. J. Physiol.* 249:G464–G469.

Melvin, J.E., A. Moran, and R.J. Turner. 1988. The role of HCO_3^- and Na^+/H^+ exchange in the response of rat parotid acinar cells to muscarinic stimulation. *J. Biol. Chem.* 263:19564–19569.

Moore, M.L., J.N. George, and R.J. Turner. 1995. Anion dependence of bumetanide binding and ion transport by the rabbit parotid Na^+-K^+-$2Cl^-$ co-transporter: evidence for an intracellular anion modifier site. *Biochem. J.* 309:637–642.

Mueller, P., and D.O. Rudin. 1967. Development of K^+-Na^+ discrimination in experimental bimolecular lipid membranes by macrocyclic antibiotics. *Biochem. Biophys. Res. Commun.* 26:398–404.

Niisato, N., Y. Ito, and Y. Marunaka. 1999. Activation of Cl^- channel and $Na^+/K^+/2Cl^-$ cotransporter in renal epithelial A6 cells by flavonoids: genistein, daidzein, and apigenin. *Biochem. Biophys. Res. Commun.* 254:368–371.

Park, K., R.L. Evans, G.E. Watson, K. Nehrke, L. Richardson, S.M. Bell, P.J. Schultheis, A.R. Hand, G.E. Shull, and J.E. Melvin. 2001a. Defective fluid secretion and NaCl absorption in the parotid glands of Na^+/H^+ exchanger-deficient mice. *J. Biol. Chem.* 276:27042–27050.

Park, M.K., R.B. Lomax, A.V. Tepikin, and O.H. Petersen. 2001b. Local uncaging of caged Ca^{2+} reveals distribution of Ca^{2+}-activated Cl^- channels in pancreatic acinar cells. *Proc. Natl. Acad. Sci. USA.* 98:10948–10953.

Paulais, M., and R.J. Turner. 1992. β-Adrenergic upregulation of the Na^+-K^+-$2Cl^-$ cotransporter in rat parotid acinar cells. *J. Clin. Invest.* 89:1142–1147.

Petersen, O.H. 1992. Stimulus-secretion coupling: cytoplasmic calcium signals and the control of ion channels in exocrine acinar cells. *J. Physiol.* 448:1–51.

Pirani, D., L.A.R. Evans, D.I. Cook, and J.A. Young. 1987. Intracellular pH in the rat mandibular salivary gland: the role of Na-H and Cl-HCO_3 antiports in secretion. *Pflugers Arch.* 408:178–184.

Poronnik, P., M.C. Ward, and D.I. Cook. 1992. Intracellular Ca^{2+} release by flufenamic acid and other blockers of the non-selective cation channel. *FEBS Lett.* 296:245–248.

Putney, L.K., C.R.T. Vibat, and M.E. O'Donnell. 1999. Intracellular Cl regulates Na-K-Cl cotransport activity in human trabecular meshwork cells. *Am. J. Physiol.* 277:C373–C383.

Robertson, M.A., and J.K. Foskett. 1994. Na^+ transport pathways in secretory acinar cells: membrane cross talk mediated by $[Cl^-]_i$. *Am. J. Physiol.* 267:C146–C156.

Robertson, M.A., M. Woodside, J.K. Foskett, J. Orlowski, and S. Grinstein. 1997. Muscarinic agonists induce phosphorylation-independent activation of the NHE-1 isoform of the Na^+/H^+ antiporter in salivary acinar cells. *J. Biol. Chem.* 272:287–294.

Russell, J.M. 2000. Sodium-potassium-chloride cotransport. *Physiol. Rev.* 80:211–276.

Smith, P.M., and D.V. Gallacher. 1992. Acetylcholine and caffeine-evoked repetitive transient Ca^{2+}-activated K^+ and Cl^- currents in mouse submandibular cells. *J. Physiol.* 449:109–120.

Soltoff, S.P., M.K. McMillian, L.C. Cantley, E.J. Cragoe Jr., and B.R. Tamalo. 1989. Effects of muscarinic, alpha-adrenergic, and substance P agonists and ionomycin on ion transport mechanisms in the rat parotid acinar cell. The dependence of ion transport on intracellular calcium. *J. Gen. Physiol.* 93:285–319.

Sugita, M., C. Hirono, S. Tanaka, T. Nakahari, Y. Imai, Y. Kanno, and Y. Shiba. 2000. Visualization of the secretory process involved in Ca^{2+}-activated fluid secretion from rat submandibular glands using the fluorescent dye, calcein. *Eur. J. Cell Biol.* 79:182–191.

Turner, R.J. 1993. Mechanisms of fluid secretion by salivary glands. *Ann. N. Y. Acad. Sci.* 694:24–35.

Turner, R.J., and J.N. George. 1988. Ionic dependence of bumetanide binding to the rabbit parotid Na/K/Cl cotransporter. *J. Membr. Biol.* 102:71–77.

Turner, R.J., and H. Sugiya. 2002. Understanding salivary fluid and protein secretion. *Oral Dis.* 8:3–11.

Wang, F., S. Zeltwanger, I.C.-H. Yang, A.C. Nairn, and T.-C. Hwang. 1998. Actions of genistein on cystic fibrosis transmembrane conductance regulator chloride channel gating. *J. Gen. Physiol.* 111: 477–490.

Zeng, W., M.G. Lee, and S. Muallem. 1997. Membrane-specific regulation of Cl^- channels by purinergic receptors in rat submandibular gland acinar and duct cells. *J. Biol. Chem.* 272:32956–32965.